Hydrocarbon activation by "bare" uranium cations: formation of a cationic uranium–benzene complex from three ethylene units ☆

Christoph Heinemann, Hans H. Cornehl, Helmut Schwarz *

Institut für Organische Chemie der Technischen Universität Berlin, Straße des 17. Juni 135, D-10623 Berlin, Germany

Abstract

The ability of the atomic uranium cation U^+ to activate a variety of saturated and unsaturated hydrocarbon molecules is investigated. Both C–H and C–C bond activation processes proceeds at markedly higher kinetic efficiencies compared with the lower congener Nd^+ from the lanthanide series. Formation of a cationic uranium–benzene complex occurs in three consecutive dehydrogenation reactions between U^+ and ethylene. The mechanism of this metal-mediated cyclotrimerization is enlightened by kinetic measurements, collision-induced dissociation experiments and ion–molecule reactions of the intermediate species.

Keywords: Gas-phase organometallic chemistry; C–H, C–C bond activation; C–C coupling; Benzene complexes; Actinides

1. Introduction

Gas-phase chemistry of "bare" and ligated transition metal cations is a rapidly developing area of research focusing on the fundamental understanding of organometallic reaction mechanisms [1]. In the absence of solvents, surfaces and other "bulk" effects the chemistry which occurs under single-collision conditions between a singly charged transition metal cation M^+ and an organic substrate (typically, a simple or a monofunctionalized hydrocarbon molecule) reflects the intrinsic reactivity of an organometallic species. Over the last few decades an extensive body of information has become available [2] and, besides well-known reaction patterns from solution-phase chemistry, new and fascinating organometallic reaction types (e.g. remote functionalization [3], and cluster-assisted C–H and C–C bond activation [4]) have been uncovered to exist in the gas phase.

Most organometallic reactivity studies in the gas phase considered cations of the first (3d block) and second (4d block) transition metal rows. Recently, also the heavier 5d block elements have attracted considerable attention. Their unique ability to activate notoriously unreactive molecules such as methane [5] and even carbon dioxide [6] has invoked new impetus to gas-phase studies of heavy elements, in particular with regard to potential mechanistic implications for "real-life" catalytic processes. Accompanying theoretical work has related the peculiar features of 5d block transition metal cation chemistry to the influence of relativistic effects, which for example enhance the Pt^+–CH_2 bond strength by as much as 50 kcal mol^{-1} [7]. With this background, we have recently carried out the first systematic investigation on the organometallic gas-phase chemistry of the 4f block or "rare earth" cations [8]. The conclusion which could be drawn after comparing the reactions of the lanthanide cations Ln^+ with a series of ten different hydrocarbon substrates was that the general reactivity decreased with increasing energy demand for the excitation of a 4f electron into either a 5d or the 6s orbital. This result confirms the well-known qualitative guideline of inorganic chemistry that electrons in the spatially compact 4f orbitals are chemically inactive. The involvement of excited electronic configurations in the gas-phase reactivity of lanthanide elements can be regarded as another reflection of relativistic influences, namely spin–orbit coupling, which provides an efficient mechanism for transitions

---

☆ Dedicated to Professor Herbert Schumann on the occasion of his 60th birthday.
* Corresponding author.

between ground- and excited-state potential energy surfaces [8a]. Other interesting chemical features of lanthanide cations in the gas phase concern their ability to activate selectively carbon–fluorine bonds [9] or to assist the oxidative dimerization of two propene molecules to benzene [10].

Here, we present an extension of these investigations to uranium, the chemically most important actinide (5f row) element. Gas-phase chemistry of "bare" U^+ cations has so far been only briefly investigated [11]. Some interesting observations made in these studies (e.g. the high proton affinity of the neutral U atom [12] or the ability of U^+ to activate CO_2 [13]) prompted us to investigate the chemical behavior of U^+ towards hydrocarbons in some more detail. The first part of this work describes the general ability of the atomic uranium cation U^+ to activate a series of unfunctionalized hydrocarbon molecules. In the second part we present a mechanistic study for the consecutive trimerization of three ethylene molecules to an intact benzene moiety, which is promoted by the U^+ cation. Since the pioneering work of Ziegler and Natta, the oligomerization of small unsaturated hydrocarbons constitutes a challenge for organometallic chemistry in general. The high activity of organolanthanide complexes of the type $Cp_2^* Ln-H$ ($Cp^* = C_5Me_5$; Ln = lanthanide) in the polymerization of ethylene under solution-phase conditions has been demonstrated in a landmark contribution by Schumann and coworkers [14] in 1985. Catalytic and stoichiometric C–C bond formation has also been reported upon reaction of molecular organometallic solids with gaseous ethyne and ethene [15]. In the gas phase, Ti^+-mediated oligomerization of up to 20 ethylene units has been reported under pressure conditions of about 0.5 mbar [16]. Under similar conditions, Ti^+-mediated oligomerization of isobutene yields polymeric organic ions of the type $C_4H_9^+(C_4H_8)_n$ [17]. The experimental set-up employed in the present work is Fourier transform (FT) ion cyclotron resonance (ICR) mass spectrometry (MS), which is typically carried out at much lower pressures of about 10^{-8} mbar, thus allowing only for the observation of the first steps of an oligomerization process on a reasonable time scale. However, such low pressure experiments will provide insight in the general principles of metal-assisted carbon-carbon bond formation, irrespective of site- and phase-specific external perturbations.
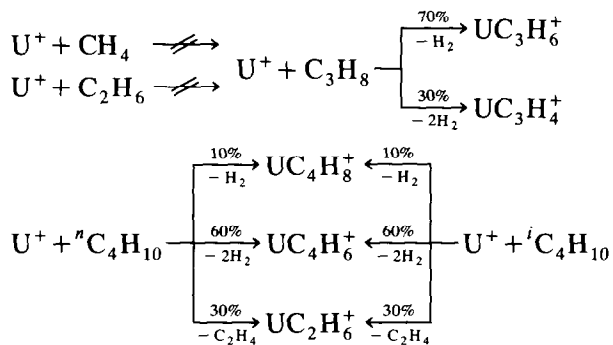
2. Experimental details

The experiments were performed using a previously described [18] Spectrospin CMS-47X FT ICR machine which is equipped with an external ion source. For ion generation by laser desorption (LD)–laser ionization (LI), the beam of a Nd-doped yttrium aluminum garnet

laser (Spectron Systems; $\lambda = 1064$ nm) was focused onto a uranium metal piece. The ions were extracted from the source and transferred to the cylindrical ICR cell by a system of electrostatic potentials and lenses. After deceleration, the ions were trapped in the field of a superconducting magnet (Oxford Instruments; maximum field, 7.05 T). The $^{238}U^+$ ion was isolated from the simultaneously generated UO_x^+ species ($x = 1, 2$) owing to surface oxidation using FERETS [19], a computer-controlled ion ejection protocol which combines frequency sweeps and single-frequency pulses to optimize ion isolation. Special care was taken to ensure thermalization of the ions prior to chemical reactions. This was affected by removal of excess energy via collisions with pulsed-in argon (maximum pressure, about 5×10^{-5} mbar for about 1 s). Uranium–ligand complexes UL^+ were generated from thermalized uranium cations by applying a short pulse of a reactant gas into the cell and isolating the desired ion using FERETS. For all reactivity studies, the reactants were admitted to the cell via a leak valve at a stationary pressure of $(1–5) \times 10^{-8}$ mbar. Reaction products were identified using high resolution mass spectra, and their reaction pathways were investigated by MS–MS and double-resonance techniques. Collision-induced dissociation (CID) experiments were carried out by (i) isolation of the desired ion using FERETS, (ii) thermalization by pulsed-in argon, (iii) kinetic excitation of this ion by an r.f. pulse and (iv) trapping it for 1 s in argon at a static pressure of 1×10^{-8} mbar. The "low energy" CID spectra refer to an excitation energy range in which the lowest energy fragmentation channels of a given ion occur. The appearance region of additional CID products will be denoted the "high energy" CID regime. Rate constants were determined from the pseudo-first-order decay of the reactant ion and are reported with an estimated accuracy of $\pm 30\%$. In cases where undesired oxidation reactions of U^+ cations of UL^+ complexes with background water or oxygen accounted for more than 5% of the product ions, the overall reaction rates were multiplied by the initial quota of C–H and C–C bond activation to obtain the correct rates for these processes. Relative reaction efficiencies are reported as percentages of the measured rate constants with respect to the theoretical collision rate k_{capt}, calculated from capture rate theory [20]. All functions of the mass spectrometer were controlled with a Bruker Aspect 3000 minicomputer.

3. Results and discussion

3.1. Gas-phase reactivity of U^+ with hydrocarbons

Scheme 1 and Table 1 provide an overview of the product ion distributions and reaction rate constants

$$U^+ + CH_4 \;\not\rightarrow\;$$
$$U^+ + C_2H_6 \;\not\rightarrow\; U^+ + C_3H_8 \underset{-2H_2}{\overset{70\%}{\xrightarrow{-H_2}}} UC_3H_6^+$$
$$\underset{-2H_2}{\overset{30\%}{\xrightarrow{\hspace{1cm}}}} UC_3H_4^+$$

$$U^+ + {}^nC_4H_{10} \underset{\substack{60\% \\ -2H_2}}{\overset{\substack{10\% \\ -H_2}}{\xrightarrow{\hspace{1cm}}}} \begin{array}{c} \xrightarrow[-H_2]{10\%} UC_4H_8^+ \xleftarrow[-H_2]{10\%} \\ \xrightarrow[-2H_2]{60\%} UC_4H_6^+ \xleftarrow[-2H_2]{60\%} \\ \xrightarrow[-C_2H_4]{30\%} UC_2H_6^+ \xleftarrow[-C_2H_4]{30\%} \end{array} U^+ + {}^iC_4H_{10}$$

Scheme 1.

determined for the gas-phase reactions between the "bare" U^+ cation and several hydrocarbons.
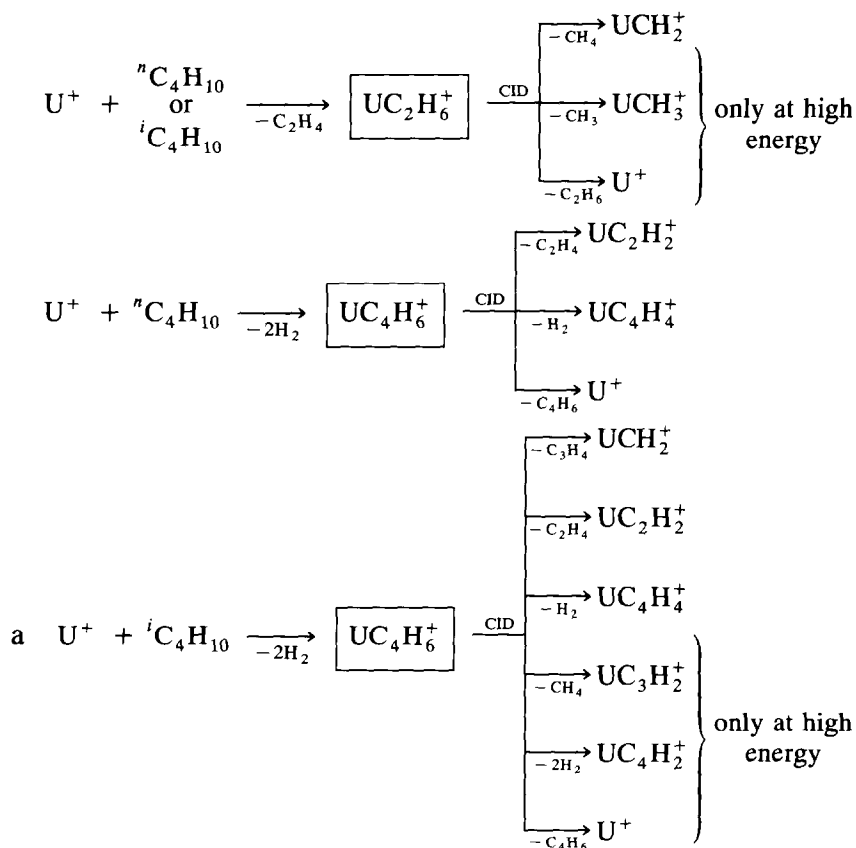
As in our previous study [8a], a series of organic substrates was chosen such that both kinetic and thermodynamic restrictions for an activation process are lowered step by step. From the observed product ions it appears that in general C–H bond activation processes predominate over C–C bond activation processes in the gas-phase reactions of U^+. In detail, both methane and ethane are unreactive with U^+ cations. For propane, one observes very slow single ($UC_3H_6^+$, 70%) and double dehydrogenation ($UC_3H_4^+$, 30%). The two butane iso-

Table 1
Absolute rate constant k_{abs} and relative rate constant k_{rel} for reactions of U^+ cations with hydrocarbons

Substrate	k_{abs} $(cm^3\,s^{-1}\,molecule^{-1})$	k_{rel} $(\% \text{ of } k_{capt})$
CH_4	$< 2 \times 10^{-12}$	< 0.002
C_2H_6	$< 3 \times 10^{-12}$	< 0.003
C_3H_8	2×10^{-11}	0.02
$n\text{-}C_4H_{10}$	2×10^{-10}	0.2
$^iC_4H_{10}$	2×10^{-10}	0.2
C_2H_2	$< 3 \times 10^{-12}$	< 0.003
C_2H_4	10×10^{-10}	1.0
$CH_2{=}CH{-}CH_3$	10×10^{-10}	1.0
$c\text{-}C_3H_6$	8×10^{-10}	0.9
$CH_2{=}CH{-}CH_2CH_3$	9×10^{-10}	0.9
$CH_2{=}CH{-}CH{=}CH_2$	10×10^{-10}	1.0
C_6H_6	9×10^{-10}	0.9

mers give rise to identical product ion distributions upon reaction with U^+. Besides single (10%) and double (60%) dehydrogenation, the $UC_2H_6^+$ ions (30%) formed in this reaction indicate the existence of an additional C–C bond activation channel. The CID spectra of the $UC_2H_6^+$ species (Scheme 2), generated from either n-butane or isobutane exhibit very similar fragmentation patterns as a function of increasing excitation energy: CH_4 loss as the lowest energy channel, fol-
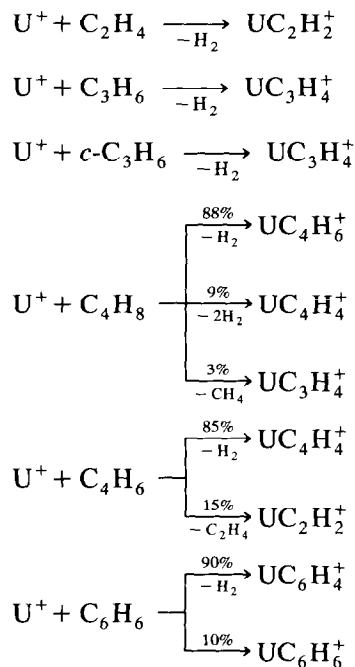
$$U^+ + \begin{array}{c} {}^nC_4H_{10} \\ \text{or} \\ {}^iC_4H_{10} \end{array} \xrightarrow[-C_2H_4]{} \boxed{UC_2H_6^+} \xrightarrow{\text{CID}} \left. \begin{array}{c} \xrightarrow[-CH_4]{} UCH_2^+ \\ \xrightarrow[-CH_3]{} UCH_3^+ \\ \xrightarrow[-C_2H_6]{} U^+ \end{array} \right\} \begin{array}{c} \text{only at high} \\ \text{energy} \end{array}$$

$$U^+ + {}^nC_4H_{10} \xrightarrow[-2H_2]{} \boxed{UC_4H_6^+} \xrightarrow{\text{CID}} \begin{array}{c} \xrightarrow[-C_2H_4]{} UC_2H_2^+ \\ \xrightarrow[-H_2]{} UC_4H_4^+ \\ \xrightarrow[-C_4H_6]{} U^+ \end{array}$$

$$\text{a}\quad U^+ + {}^iC_4H_{10} \xrightarrow[-2H_2]{} \boxed{UC_4H_6^+} \xrightarrow{\text{CID}} \left. \begin{array}{c} \xrightarrow[-C_3H_4]{} UCH_2^+ \\ \xrightarrow[-C_2H_4]{} UC_2H_2^+ \\ \xrightarrow[-H_2]{} UC_4H_4^+ \\ \xrightarrow[-CH_4]{} UC_3H_2^+ \\ \xrightarrow[-2H_2]{} UC_4H_2^+ \\ \xrightarrow[-C_4H_6]{} U^+ \end{array} \right\} \begin{array}{c} \text{only at high} \\ \text{energy} \end{array}$$

Scheme 2.

lowed by loss of a CH_3 radical, and finally regeneration of the "bare" metal cation. For other metal cations M^+, similar results have been interpreted as indicative of cationic dimethyl structures $M(CH_3)_2^+$ (e.g. $M = Sc$ [21], Y [22] or La [22]). However, while the mechanistic picture for the generation of $M(CH_3)_2^+$ from n-butane is straightforward [2d,21a], its formation from isobutane requires a substantial rearrangement of the carbon skeleton.

In contrast, the CID spectra of the double dehydrogenation product $UC_4H_6^+$ differ characteristically when generated from either n-butane or isobutane. For the $UC_4H_6^+$ ion derived from n-butane, loss of C_2H_4 and of the entire C_4H_6 unit dominate the low energy CID processes, together with some contributions from an H_2-loss channel. No additional CID products appear when the excitation energy is increased within the usual range applied in this study. Generated from isobutane as the neutral precursor, the $UC_4H_6^+$ cation loses preferentially C_3H_4, C_2H_4 and H_2 in the low energy regime, with additional losses of methane, the entire C_4H_6 ligand and two H_2 molecules occurring at higher energies. The comparison of these data shows that, in contrast with the C–C bond activation reaction, the uranium-mediated double dehydrogenation of n-butane and isobutane leads to at least two different $UC_4H_6^+$ isomers. However, their structures cannot be assigned on the basis of the CID data, since rearrangements between several minima on the relevant potential energy surfaces may occur prior to dissociation on the time and energy scales of the experiments. However, in analogy to earlier studies of CID spectra of $MC_4H_6^+$ ions ($M = Y$ [22], La [22] or Ce [10]) generated from n-butane and isobutane it is reasonable to interpret the fragmentation patterns in terms of the cationic metal complexes of butadiene and trimethylenemethane respectively.

As expected, the reaction rates increase in the sequence CH_4, C_2H_6, C_3H_8 and C_4H_{10}. This is due to the larger polarizabilities of the higher hydrocarbon molecules which deepen the U^+–C_nH_{2n+2} interaction potential. As a consequence the lifetimes of the ion–molecule encounter complexes, which are initially formed in the course of any ion–molecule reaction, increase with increasing size of the alkane. Moreover, the deeper potential well provides a larger amount of energy to overcome possible activation barriers associated with C–H and C–C bond activation. However, the observed inertness of CH_4 and C_2H_6 towards U^+ might also be due to additional thermodynamic restrictions associated with the necessary scission of two primary C–H bonds.

Compared with the alkane reactions, all unsaturated hydrocarbon molecules investigated in this study but acetylene are found to be very reactive with "bare" uranium cations (Table 1 and Scheme 3). In the case of acetylene no reaction with U^+ was observed.

$$U^+ + C_2H_4 \xrightarrow[-H_2]{} UC_2H_2^+$$

$$U^+ + C_3H_6 \xrightarrow[-H_2]{} UC_3H_4^+$$

$$U^+ + c\text{-}C_3H_6 \xrightarrow[-H_2]{} UC_3H_4^+$$

$$U^+ + C_4H_8 \begin{cases} \xrightarrow[-H_2]{88\%} UC_4H_6^+ \\ \xrightarrow[-2H_2]{9\%} UC_4H_4^+ \\ \xrightarrow[-CH_4]{3\%} UC_3H_4^+ \end{cases}$$

$$U^+ + C_4H_6 \begin{cases} \xrightarrow[-H_2]{85\%} UC_4H_4^+ \\ \xrightarrow[-C_2H_4]{15\%} UC_2H_2^+ \end{cases}$$

$$U^+ + C_6H_6 \begin{cases} \xrightarrow[-H_2]{90\%} UC_6H_4^+ \\ \xrightarrow{10\%} UC_6H_6^+ \end{cases}$$

Scheme 3.

Ethene and propene undergo kinetically efficient single dehydrogenation while, for 1-butene, small percentages of double dehydrogenation (9%) and C–C bond activation (3%, loss of CH_4) are observed. C–C bond activation of propene is not observed for thermalized U^+ cations; however, when unthermalized U^+ stemming directly from the LD–LI process is reacted with this substrate, UCH_2^+, together with additional products such as UH^+ [12], is formed [23]. Cyclopropane reacts identically with propene (exclusive formation of $UC_3H_4^+$). 1-Butene is mainly singly dehydrogenated (88%). Furthermore, some double dehydrogenation (9%) as well as loss of methane (3%) are observed. Butadiene mainly undergoes single dehydrogenation (85%) together with some contributions from a C–C bond activation channel (15% loss of ethylene). Finally, even benzene is efficiently dehydrogenated by U^+ ($UC_6H_4^+$, 90%) with concomitant formation of the corresponding adduct complex $UC_6H_6^+$ (10%). All primary $UC_xH_y^+$ product ions undergo secondary reactions with the unsaturated hydrocarbons. In the second part of this paper, it will be demonstrated for the ethylene case that these processes involve carbon–carbon bond formation.

On the basis of the observed processes we can conclude that the uranium cation U^+ (electron configuration, $7s^2 5f^3$; ground-state term symbol, $^4I_{9/2}^0$ [24]) is in general more reactive towards hydrocarbons than its lighter 4f row congener Nd^+ (ground-state electron configuration, $6s^1 4f^4$; ground-state term symbol, $^4I_{7/2}^0$ [25]). The latter was found to be unreactive with all small alkanes, ethylene, propene as well as butadiene and activates 1-butene with only moderate efficiency

[8a,26]. As shown above, U^+ does in fact activate small alkanes and exhibits 100% kinetic efficiency when reacting with unsaturated hydrocarbons. One possible explanation for this finding invokes the different natures of the 4f and 5f orbitals. Although the former are formally part of the valence shell of a lanthanide cation, they are known to be spatially compact, which is the reason for their chemical inertness [27]. Accordingly, it was found that a minimum of 2 non-f (i.e. 5d or 6s) electrons is required for a lanthanide cation to activate an alkane under FT ICR conditions [8a]. Pictorially, one might imagine these two electrons to interact with the antibonding orbital of the initially attacked C–H bond of the substrate in the primary step. In this simple one-electron picture (the closed $7s^2$ shell is not expected to be "inert" with regard to C–H bond activation [8a]), it is possible to interpret the experimental data for hydrocarbon activation by U^+ cations in the sense that the 5f electrons are indeed able to bring about C–H bond activation, while the 4f electrons are not. This conclusion is in line with the general notion that 5f orbitals at the beginning of the actinide series are in fact part of the valence shell in the sense that their spatial extent is similar to their 7s and 6d congeners [28]. In addition, U^+ has a number of energetically low lying excited states deriving from the $5f^3 6d^1 7s^1$ configuration (e.g. the $^6L^0_{11/2}$, +0.9 kcal mol^{-1} [24]) which might contribute to the observed reactivity because they are thermally populated either under the conditions of the FT ICR experiment or via a spin–orbit-mediated curve-crossing mechanism as discussed earlier [8a]. To differentiate between these two scenarios for the question of 5f electron reactivity would require an comprehensive data basis (as in the lanthanide series [8a]) for the reactions of actinide cations with a series of hydrocarbon substrates, which is not feasible in our laboratory owing to the radioactive nature of the 5f elements.

3.2. Trimerization of ethylene promoted by U^+ cations

The primary reaction product in the U^+–C_2H_4 system corresponds to a complex of the composition $UC_2H_2^+$. A secondary reaction of this ion with ethylene affords the species $UC_4H_4^+$, which once more dehydrogenates ethylene to form $UC_6H_6^+$ as the only reaction product (Scheme 4).

The rate constants for these three processes are remarkably different. While the primary activation proceeds with 100% kinetic efficiency, the second step in this triad is quite inefficient with an absolute rate con-
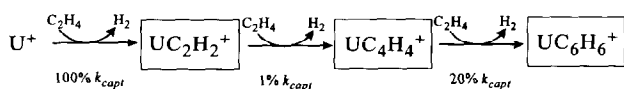
$$UC_6H_6^+ + C_6D_6 \longrightarrow UC_6D_6^+ + C_6H_6$$
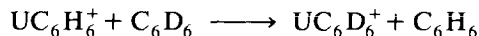
Scheme 5.

stant of 1×10^{-11} cm^3 s^{-1} molecule^{-1} (1% of the collisional limit k_{cap}). The third step is considerably faster ($k = 2 \times 10^{-10}$ cm^3 s^{-1} molecule^{-1}; 20% of the collisional limit k_{cap}); the reaction of the product ion $UC_6H_6^+$ with an additional molecule of ethylene is again an order of magnitude less efficient. In the following, a step-by-step characterization of the ion structures and the mechanisms involved in this cascade of ion–molecule reactions will be attempted.
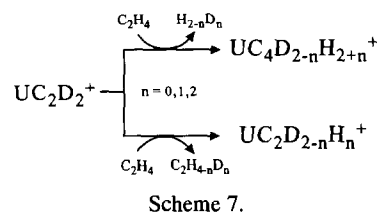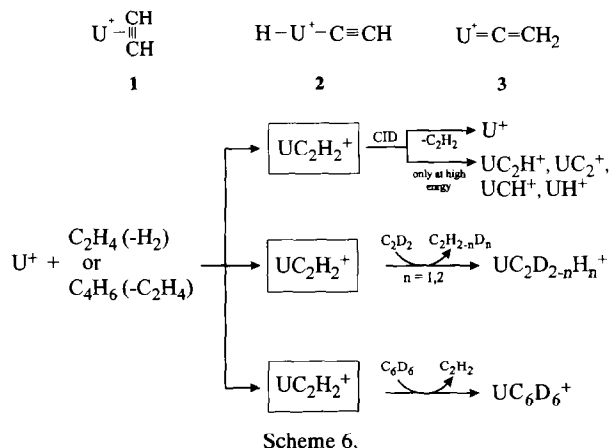
First of all, the identity of the $UC_6H_6^+$ product ion has to be established. CID of this species, generated from three molecules of ethylene, yields exclusively an atomic uranium cation at low energies. While this experiment already indicates that an intact C_6H_6 moiety has been formed in the three consecutive reactions at the metal center, this evidence is still not conclusive, since the C_6H_6 unit might possibly have been formed upon high energy excitation in the CID experiment. In order to exclude this possibility, the $UC_6H_6^+$ ion resulting from $UC_4H_4^+$ and ethylene was reacted with benzene-d_6. In fact, besides a small fraction of adduct formation ($UC_{12}H_6D_6^+$), exclusive substitution of the metal coordinated C_6H_6 by C_6D_6 is observed in a single-collision event (Scheme 5); this result ultimately proves that benzene has been formed at the uranium center. Earlier reports for the same reaction type under FT ICR conditions have been made for the "bare" niobium and tungsten cations and the iron cluster Fe_4^+ [29]; unfortunately, the definitive proof for benzene formation via thermoneutral ligand exchange with C_6D_6 was not given in these reports [29d]. However, definitive identification of benzene formation and Fe$^+$-mediated acetylene trimerization was given in a study using the technique of neutralization–reionization mass spectrometry [30]. The interaction of transition metal cations with benzene has also been studied theoretically over the recent years [31].

In the characterization of the ionic intermediates in this metal-mediated cyclotrimerization of ethylene, we first focus on the $UC_2H_2^+$ ion. Formally, three possible isomers have to be considered (Scheme 6): a cationic uranium–acetylene complex 1, the insertion product 2 and the vinylidene complex 3.

The CID spectrum of $UC_2H_2^+$ is dominated by the loss of C_2H_2 over the whole energy regime applied; minor processes at higher energies are due to the elimination of H', H_2, CH' and C_2H' respectively, yielding the corresponding ions UC_2H^+, UC_2^+, UCH^+ and UH^+. Since interconversion between the structures 1–3 upon collision of $UC_2H_2^+$ with an argon atom cannot be excluded a priori, the CID results remain ambiguous. However, in the case of structure 3 in addition to the
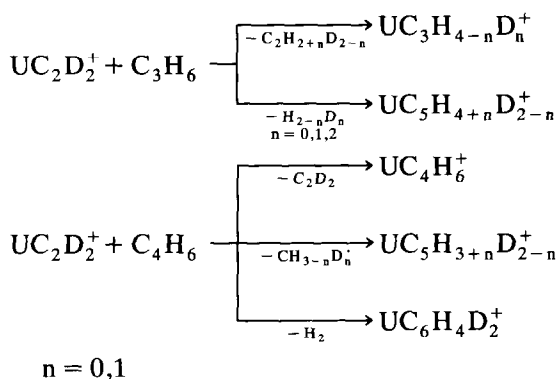
$$U^+ \xrightarrow[\text{100\% } k_{cap}]{C_2H_4 \quad H_2} \boxed{UC_2H_2^+} \xrightarrow[\text{1\% } k_{cap}]{C_2H_4 \quad H_2} \boxed{UC_4H_4^+} \xrightarrow[\text{20\% } k_{cap}]{C_2H_4 \quad H_2} \boxed{UC_6H_6^+}$$

Scheme 4.

$$U^+\overset{CH}{\underset{CH}{-\|\|}} \qquad H-U^+-C\equiv CH \qquad U^+=C=CH_2$$

$$\mathbf{1} \qquad\qquad\qquad \mathbf{2} \qquad\qquad\qquad \mathbf{3}$$

Scheme 6 (left):

$$U^+ + \begin{array}{c} C_2H_4\ (-H_2)\\ \text{or}\\ C_4H_6\ (-C_2H_4) \end{array} \longrightarrow$$

$$\boxed{UC_2H_2^+} \xrightarrow[\text{only at high energy}]{\text{CID} -C_2H_2} \begin{array}{l} U^+ \\ UC_2H^+, UC_2^+, \\ UCH^+, UH^+ \end{array}$$

$$\boxed{UC_2H_2^+} \xrightarrow[n=1,2]{C_2D_2 \quad C_2H_{2-n}D_n} UC_2D_{2-n}H_n^+$$

$$\boxed{UC_2H_2^+} \xrightarrow{C_6D_6 \quad C_2H_2} UC_6D_6^+$$

Scheme 6.

Scheme 7 (right):

$$UC_2D_2^+ \xrightarrow[n=0,1,2]{} \begin{array}{l} \xrightarrow{C_2H_4 \quad H_{2-n}D_n} UC_4D_{2-n}H_{2+n}^+ \\ \xrightarrow{C_2H_4 \quad C_2H_{4-n}D_n} UC_2D_{2-n}H_n^+ \end{array}$$

Scheme 7.

observed fragmentations also collision-induced loss of CH_2 giving rise to a UC^+ signal is expected. Thus the absence of the latter signal points towards structures **1** and **2**. For further differentiation, ligand exchange experiments with C_2D_2 and C_6D_6 were performed (see Scheme 6). In the reaction of $UC_2H_2^+$ with C_2D_2 the products $UC_2D_2^+$ (70%) and UC_2HD^+ (30%) were generated. While this result is still somewhat inconclusive, the ligand exchange of $UC_2H_2^+$ with C_6D_6 yields $UC_6D_6^+$ exclusively, in an efficient exothermic reaction process. Since substitution of the covalently bonded vinylidene ligand in **3** by benzene would be a slow or even endothermic process, we conclude that the $UC_2H_2^+$ species, generated from "bare" U^+ and ethylene, corresponds to either a cationic metal–acetylene **1** or, less likely, the isomeric hydrodo-ethynyl structure **2**. A further and definitive distinction between **1** and **2** is not possible since both isomers might easily undergo H–D exchange in the $UC_2H_2^+$–C_2D_2 collision complex. In other words, complexation of C_2D_2 to $UC_2H_2^+$ may induce rearrangements between structures **1** and **2** [4a] such that the observed product ions do no longer provide structure-indicative information about the $UC_2H_2^+$ reactant. We note in passing that the ligand exchange as well as the CID experiments give identical results when $UC_2H_2^+$ is generated from either C_2H_4 or C_4H_6 (see Scheme 1). Thermochemical and theoretical data for a variety of other $MC_2H_2^+$ species are available in the literature [32].

In the secondary reaction of the $UC_2H_2^+$ ion with ethylene, only 1% of all collisions give rise to the formation of $UC_4H_4^+$. However, if $UC_2D_2^+$ is reacted with C_2H_4, rapid H–D exchange in the reactant ion occurs together with formation of all possible $UC_4D_{2-n}H_{2+n}^+$ isotopomers ($n = 0, 1, 2$ (Scheme 7)). The rate constant for the sum of these processes corresponds to the gas kinetic collision rate. This suggests that C–H bond activation occurs upon every collision of the cationic uranium–acetylene complex with a C_2H_4 molecule. The low branching ratio for the $UC_4H_4^+$

product channel is an indication that the first acetylene molecule is more than a "spectator" ligand (see below). Obviously, formation of $UC_4H_4^+$ from $UC_2H_2^+$ and C_2H_4 involves a more complicated sequence of elementary steps than a simple dehydrogenation of ethylene, which occurs, as described above, with 100% kinetic efficiency for "bare" U^+ cations.
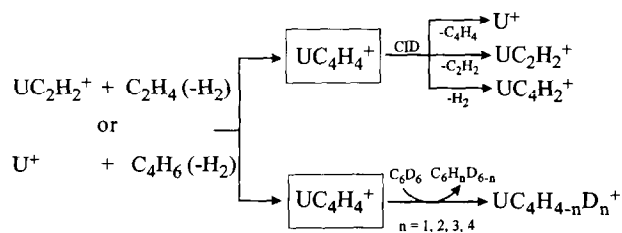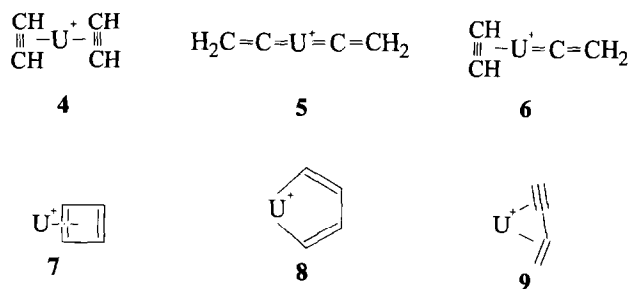
In contrast with the ethylene case, dihydrogen, methane and ethane were found to be completely unreactive with $UC_2D_2^+$. However, kinetically efficient reactions with other unsaturated hydrocarbons do occur, with propene, both $UC_3H_{4-n}D_n^+$ ($n = 0, 1, 2$ with a $1:2:1$ ratio) and $UC_5H_{4+n}D_{2-n}^+$ ($n = 0, 1, 2$ with a $10:2:1$ ratio) are formed as depicted in Scheme 8. In the reaction with 1,3-butadiene we observe, besides ligand exchange (which is yet another indication for the metal–acetylene structure **1**), the formation of $UC_5H_{3+n}D_{2-n}^+$ ($n = 0, 1$ in a $2:1$ ratio) and $UC_6H_4D_2^+$ are observed (see Scheme 8). Upon CID, the lowest energy fragmentation of $UC_5H_5^+$, generated from unlabelled $UC_2H_2^+$ and propene, results in the formation of the atomic U^+ cation, and additional $UC_3H_n^+$ species ($n = 1, 2, 3$) are observed at higher energies. Moreover, $UC_5H_5^+$ does not undergo ligand exchange with C_6D_6 (only formation of the $UC_{11}H_5D_6^+$ adduct was observed) which suggests, on the basis of the results for $UC_2H_2^+$, that the structure of the $UC_5H_5^+$ ions comprises an intact C_5H_5 moiety. No H–D exchange in the $UC_2D_2^+$ reactant ion is observed in the reactions with propene and 1,3-butadiene, in sharp contrast with the kinetically inefficient reaction of $UC_2D_2^+$ with ethylene.

We next focus on the identity of the $UC_4H_4^+$ species (Scheme 9). In principle, the structure of this ion may correspond either to two separate ligands attached to the

Scheme 8:

$$UC_2D_2^+ + C_3H_6 \longrightarrow \begin{array}{l} \xrightarrow{-C_2H_{2+n}D_{2-n}} UC_3H_{4-n}D_n^+ \\ \xrightarrow[n=0,1,2]{-H_{2-n}D_n} UC_5H_{4+n}D_{2-n}^+ \end{array}$$

$$UC_2D_2^+ + C_4H_6 \longrightarrow \begin{array}{l} \xrightarrow{-C_2D_2} UC_4H_6^+ \\ \xrightarrow{-CH_{3-n}D_n} UC_5H_{3+n}D_{2-n}^+ \\ \xrightarrow{-H_2} UC_6H_4D_2^+ \end{array}$$

$$n = 0, 1$$

Scheme 8.

Scheme 9.

U$^+$ cation, i.e. the bis(acetylene) structure **4**, a bis(vinylidene) species **5** or a mixed acetylene–vinylidene complex **6**; other conceivable isomers may contain a cyclobutadiene ligand (**7**) or correspond to a metallacyclopentadiene species **8**, and even the linear but-1-yne-3-ene complex **9** cannot be ruled out a priori. Upon CID, three equally important reaction channels with losses of H_2, C_2H_2 and C_4H_4 from $UC_4H_4^+$ are observed. Again, more useful information is provided by the ligand-exchange experiment with C_6D_6, in which no formation of $UC_6D_6^+$, but rather fast H–D scrambling in $UC_4H_4^+$ is observed (see Scheme 9).

This observation obviously rules out structures **4** and **6** with intact or inserted acetylene moieties, since these can easily be replaced by a benzene ligand as shown above for $UC_2H_2^+$. On similar grounds also a cyclobutadiene structure **7** seems improbable. An acetylene → vinylidene rearrangement of the first ligand during the secondary reaction of $UC_2H_2^+$ with C_2H_4 is required for the formation of structure **5**. Such processes are known to be facilitated in the presence of a transition metal center [33]. However, the assumption of either structure **8** or structure **9** is more in line with the largely differing rates between the secondary and the tertiary reaction steps in the benzene formation by trimerization of ethylene at the atomic U$^+$ metal center. Several quite complicated elementary steps with potentially low reaction efficiencies due to energy barriers and entropic bottlenecks are required for C–C bond formation in the $UC_2H_2^+$–C_2H_4 collision complex leading to either **8** or **9**. These two structures may easily interconvert via U$^+$-mediated 1,3-hydrogen shifts and it appears questionable whether a formal distinction between a σ-bonded metallacycle and a π-bonded ene-yne complex meets the structural and dynamic characteristics of the

observed ionic species on the $[U,C_4,H_4]^+$ potential energy surface under the experimental conditions at all. If such an intact C_4H_4 intermediate is once generated, the terminal carbon atoms of the C_4 skeleton are already activated, thus providing an easy entry for the efficient coupling of the final two C–C bonds required for benzene formation in the third reaction step. For the bis(vinylidene) isomer **5**, one would rather expect the reverse order of reaction efficiencies, namely first the fast activation of the second ethylene molecule and a subsequent metal-mediated cycloaddition upon reaction of $UC_4H_4^+$ with the third ethylene molecule. This hypothetic $C_2 + C_2 + C_2$ coupling is most probably associated with substantial energetic and entropic restrictions and not compatible with the observed reactivity pattern. Thus, on the basis of the kinetic data for U$^+$-mediated benzene formation from three ethylene units, we exclude structure **5** for the $UC_4H_4^+$ ion. Summarizing, these results leave the isomeric structures **8** and **9**, in which the C_4H_4 moiety corresponds to one intact ligand, as the most probable structures for the $UC_4H_4^+$ ion. In comparable mechanistic studies in the condensed phase, substituted metallacyclopentadiene structures were identified and found to react with acetylene derivatives to form a benzene unity [34]. All experimental results described so far for the $UC_4H_4^+$ species formed from two ethylene unities hold true as well for the identically composed species generated upon dehydrogenation of butadiene by U$^+$ cations; this is yet another argument for the presence of an intact C_4 skeleton in $UC_4H_4^+$.

4. Conclusions

In this paper an overview of the reactivity of a U$^+$ cation towards small saturated and unsaturated hydrocarbons is given. As for the alkanes under investigation the C–H and C–C bond activation patterns observed parallel the results obtained earlier [8a] for the most reactive lanthanide cations La$^+$, Ce$^+$ and Gd$^+$. All alkenes employed here, as well as cyclopropane, react very efficiently upon collision with U$^+$. In comparison, U$^+$ exhibits a far more rich chemistry than its lower congener of the 4f series, i.e. Nd$^+$. This observation is explained in terms of the greater spatial extension of the 5f relatively to the 4f orbitals. Thus 5f electrons as part of the chemically active valence shell can be involved in primary bond insertion processes.

Furthermore, a stepwise oligomerization of ethylene at the cationic U$^+$ center to form a U$^+$–benzene complex was studied in detail. The observed dramatic changes in reaction rates from one step to the next can be related to different structures of the intermediates. Activation and insertion of the second ethylene molecule

obviously represent the bottleneck of the overall process. A U^+–acetylene complex as primary reaction product dehydrogenates ethylene to form, after a complex rearrangement including C–C coupling, a metallacycle that is finally able to insert a third C_2 unit to generate the benzene ligand.

Acknowledgments

References and notes

[1] (a) D.H. Russell (ed), *Gas Phase Inorganic Chemistry*, Plenum, New York, 1988; (b) A. Fontijn (ed.), *Gas-Phase Metal Reactions*, North-Holland, Amsterdam, 1992.

[2] For recent reviews see: (a) P.B. Armentrout and J.L. Beauchamp, *Acc. Chem. Res.*, 22 (1989) 315; (b) J.A. Martinho Simões and J.L. Beauchamp, *Chem. Rev.*, 90 (1990) 629; (c) P.B. Armentrout, *Annu. Rev. Phys. Chem.*, 41 (1991) 313; (d) K. Eller and H. Schwarz, *Chem. Rev.*, 91 (1991) 1121; (e) J.C. Weishaar, *Acc. Chem. Res.*, 26 (1993) 213; (f) B.S. Freiser, *Acc. Chem. Res.*, 27 (1994) 353.

[3] H. Schwarz, *Acc. Chem. Res.*, 22 (1989) 282.

[4] (a) J.E. Bushnell, P.R. Kemper, P. Maitre and M.T. Bowers, *J. Am. Chem. Soc.*, 116 (1994) 9710; (b) P.A.M. van Koppen, P.R. Kemper, J.E. Bushnell and M.T. Bowers, *J. Am. Chem. Soc.*, 117 (1995) 2098.

[5] (a) K.K. Irikura and J.L. Beauchamp, *J. Phys. Chem.*, 95 (1991) 8344; (b) R. Wesendrup, D. Schröder and H. Schwarz, *Angew. Chem., Int. Edn. Engl.*, 33 (1994) 223; (c) C. Heinemann, R. Wesendrup and H. Schwarz, *Chem. Phys. Lett.*, 239 (1995) 75.

[6] R. Wesendrup and H. Schwarz, *Angew. Chem.*, in press.

[7] C. Heinemann, R.H. Hertwig, R. Wesendrup, W. Koch and H. Schwarz, *J. Am. Chem. Soc.*, 117 (1995) 495.

[8] (a) H.H. Cornehl, C. Heinemann, D. Schröder and H. Schwarz, *Organometallics*, 14 (1995) 992; (b) For related work in this context see: J.B. Schilling and J.L. Beauchamp, *J. Am. Chem. Soc.*, 110 15; (1988) (c) W.W. Yin, A.G. Marshall, J. Marçalo and A. Pires de Matos, *J. Am. Chem. Soc.*, 116 (1994) 8666.

[9] C. Heinemann, N. Goldberg, I. Tornieporth-Oetting, T.M. Klapötke and H. Schwarz, *Angew. Chem., Int. Edn. Engl.*, 34 (1995) 213.

[10] C. Heinemann, D. Schröder and H. Schwarz, *Chem. Ber.*, 127 (1994) 1807.

[11] (a) P.B. Armentrout and J.L. Beauchamp, *J. Phys. Chem.*, 85 (1981) 4103; (b) Z. Liang, A.G. Marshall, A. Pires de Matos and J.C. Spirlet, in L.A. Morss and J. Fuger (eds.), *Transuranium Elements — A Half Century*, American Chemical Society, Washington, DC, 1992.

[12] (a) P.B. Armentrout, R. Hodges and J.L. Beauchamp, *J. Am. Chem. Soc.*, 99 (1977) 3162. (b) P.B. Armentrout, R. Hodges and J.L. Beauchamp, *J. Chem. Phys.*, 66 (1977) 4683.

[13] C. Heinemann and H. Schwarz, *Chem. Eur. J.*, 1 (1995) 7.

[14] (a) G. Jeske, H. Lauke, H. Mauermann, P.N. Swepston, H.

Schumann and T.J. Marks, *J. Am. Chem. Soc.*, 107 (1985) 8091; (b) G. Jeske, L.E. Schock, P.N. Swepston, H. Schumann and T.J. Marks, *J. Am. Chem. Soc.*, 107 (1985) 8103; (c) G. Jeske, H. Lauke, H. Mauermann, H. Schumann and T.J. Marks, *J. Am. Chem. Soc.*, 107 (1985) 8111.

[15] C. Bianchini, M. Graziani, J. Kaspar, A. Meli and F. Vizza, *Organometallics*, 13 (1994) 1165.

[16] B.C. Guo and A.W. Castleman, *J. Am. Chem. Soc.*, 114 (1992) 6152.

[17] G.M. Daly and M.S. El-Shall, *J. Phys. Chem.*, 98 (1994) 696.

[18] (a) K. Eller and H. Schwarz, *Int. J. Mass Spectrom. Ion Processes*, 93 (1989) 243; (b)K. Eller, W. Zummack and H. Schwarz, *J. Am. Chem. Soc.*, 112 (1990) 621.

[19] R.A. Forbes, F.H. Laukien and J. Wronka, *Int. J. Mass Spectrom. Ion Processes*, 83 (1988) 23.

[20] T. Su and W.J. Chesnavich, *J. Chem. Phys.*, 76 (1982) 5183.

[21] (a) M.A. Tolbert and J.L. Beauchamp, *J. Am. Chem. Soc.*, 106 (1984) 8117; (b) For recent studies of $Sc(CH_3)_2^+$ see: Y. Huang, Y.D. Hill, M. Sodupe, C.W. Bauschlicher and B.S. Freiser, *J. Am. Chem. Soc.*, 114 (1992) 9106; (c) K.C. Crellin, S. Geribaldi and J.L. Beauchamp, *Organometallics*, 13 (1994) 3733.

[22] Y. Huang, M.B. Wise, D.B. Jacobson and B.S. Freiser, *Organometallics*, 6 (1987) 346.

[23] Exothermic generation of MCH_2^+ from M^+–propene has so far only been observed for M = La or Ce [10].

[24] A.A. Radzig and B.M. Smirnov, *Reference Data on Atoms, Molecules and Ions, Springer Series in Chemical Physics*, Vol. 31, Springer, Berlin, 1985. For information about details of the atomic U^+ states, see also: J. Blaise, J.-F. Wyart, J.G. Conway and E.F. Worden, *Phys. Scr.*, 22 (1980) 224.

[25] W.C. Martin, R. Zalubas and L. Hagan, *Atomic Energy Levels — The Rare Earth Elements*, in *NBS Natl. Ref. Data Ser.*, 60, 1978 (National Bureau of Standards, Washington, DC).

[26] H.H. Cornehl, C. Heinemann and H. Schwarz, 1995, unpublished results.

[27] M. Dolg, H. Stoll, A. Savin and H. Preuss, *Theor. Chim. Acta*, 75 (1989) 173.

[28] (a) M. Pepper and B.E. Bursten, *Chem. Rev.*, 91 (1991) 719; (b) B.E. Bursten and A.J. Strittmatter, *Angew. Chem.*, 103 (1991) 1085; (c) M.G. Cory, S. Köstlmeier, M. Kotzian, N. Rösch and M.C. Zerner, *J. Chem. Phys.*, 100 (1994) 1353; (d) W. Küchle, M. Dolg, H. Stoll and H. Preuss, *J. Chem. Phys.*, 100 (1994) 874.

[29] (a) For Nb^+ see: S.W. Buckner, T.J. MacMahon, G.D. Byrd and B.S. Freiser, *Inorg. Chem.*, 28 (1989) 3511; (b) For Fe_4^+ see: M.P. Irion, *Int. J. Mass Spectrom. Ion Processes*, 121 (1992) 1; (c) For W^+ see: C. Berg, S. Kaiser, C. Kronseder, G. Niedner-Schatteburg and V.E. Bondybey, *Chem. Phys. Lett.*, 231 (1994) 139; (d) recently the C_6H_6 product generated by Fe_4^+ mediated dehydrogenative trimerization of C_2H_4 has been identified as a benzene ligand using the thermoneutral ligand exchange reaction with C_6D_6: M.P. Irion, 1995, personal communication.

[30] D. Schröder, D. Sülzle, J. Hrušák, D.K. Böhme and H. Schwarz, *Int. J. Mass Spectrom. Ion Processes*, 110 (1991) 145.

[31] (a) C.W. Bauschlicher, H. Partridge and S.R. Langhoff, *J. Phys. Chem.*, 96 (1992) 3273; (b) S. Roszak and K. Balasubramanian, *Chem. Phys. Lett.*, 234 (1995) 101; (c) K. Seemeyer, R.H. Hertwig, J. Hrušák, W. Koch and H. Schwarz, *Organometallics*, in press.

[32] (a) For experimental bond energies from ion-beam studies see: L.S. Sunderlin and P.B. Armentrout, *Int. J. Mass Spectrom. Ion Processes*, 94 (1989) 149; (b) For experimental bond energies from photodissociation experiments see: D.R.A. Ranatunga and

B.S. Freiser, *Chem. Phys. Lett.*, *233* (1995) 319; (c) For theory see: M. Sodupe and C.W. Bauschlicher, *J. Phys. Chem.*, *95* (1991) 8640.

[33] (a) J.P. Collman, L.S. Hegedus, J.R. Norton and R.G. Finke, *Principles and Applications of Organotransition Metal Chemistry*, University Science Books, Mill Valley, CA, 1987; (b)

B.M. Trost, G. Dyker and R. Kulawiec, *J. Am. Chem. Soc.*, *112* (1990) 7809.

[34] (a) N.E. Schore, *Chem. Rev.*, *88* (1988) 1081; (b) M.J. Winter, in F.R. Hartley and S. Patai (eds.), *The Chemistry of the Metal–Carbon Bond*, Wiley, New York, 1985; (c) K.P.C. Vollhardt, *Acc. Chem. Res.*, *10* (1977) 1.